Talanta 105 (2013) 167–172

Contents lists available at SciVerse ScienceDirect

Talanta

journal homepage: www.elsevier.com/locate/talanta

On-line enantioseparation of chlorpheniramine using β-cyclodextrin and carbon nanotubes after multivariate optimization

Gimena Acosta [a,b], Raúl Silva [c], Raúl A. Gil [a,b], Roxana Gomez [a,b], Liliana P. Fernández [a,b,*]

[a] Área de Química Analítica, Chacabuco y Pedernera, San Luis 5700, Argentina
[b] Instituto de Química de San Luis (CCT-San Luis), Chacabuco y Pedernera, San Luis 5700, Argentina
[c] Área de Farmacotecnia, Universidad Nacional de San Luis, Chacabuco y Pedernera, San Luis 5700, Argentina

ARTICLE INFO

Article history:
Received 30 October 2012
Received in revised form
17 November 2012
Accepted 19 November 2012
Available online 2 December 2012

Keywords:
On-line enantioresolution
Carbon nanotubes
β-cyclodextrin
Flow injection analysis
Multivariate optimization

ABSTRACT

Multiwalled carbon nanotubes are evaluated here as solid phase extraction (SPE) sorbent aiming to (±)-chlorpheniramine (CPA) enantioresolution with fluorimetric detection. β-cyclodextrin (CD) was added to the racemate and solutions with HCl and sodium dodecyl sulfate (SDS) in different proportions were assayed as eluents to achieve the separation between both enantiomers. The overall methodology involved a flow injection (FI) strategy enabling high sample throughput and low reagents consumption making it suitable for drug routine quality control. An adequate enantioresolution (2.08) with satisfactory responses for both (R)-CPA (peak area=285) and (S)-CPA (peak area=380) was achieved applying the proposed FI-SPE strategy under the optimized conditions [β–CD]=1.0 mmol L^{-1}, [HCl]=1.0×10^{-2} mol L^{-1}, [SDS]=4.0×10^{-4} mol L^{-1} and eluent flow rate=8.0 rpm.

1. Introduction

The high specific surface area, nano-scale structure as well as high thermal stability of carbon nanotubes (CNTs) have allowed their application for the development of higher performance separation techniques that utilize nanoscale interactions. They exist as single-walled nanotubes (SWCNTs) or multiwalled nanotubes (MWCNTs), and well as open or close-ended structures with various morphologies and diameters. In general, their chemical synthesis is a noteworthy challenge, since their dimensions (diameter and length); alignment (zig-zag, armchair or chiral) and the number of walls should be controlled by choosing of appropriated procedure [1–3]. Considering their spatial structure, CNTs have been utilized as chiral stationary phase in chromatographic and no chromatographic methods in order to achieve enantioseparation of pharmaceutical compounds that possess at least one more chiral center [4,5]. Despite of the fact that the majority of the chiral drugs are prescribed and used as racemates, in most cases the pharmacological activity is restricted to one of the enantiomers, whereas the remaining form can show no effect or produce different therapeutic or even adverse responses [6]. Recognizing the importance of chiral effects, the Food and Drug Administration (FDA) issued a mandate in 1992 that required pharmaceutical companies to verify the enantiomeric purities of the chiral drugs that they produce [7]. This is the reason why separation of enantiomeric compounds is attracting more attention owing to the enormous importance in many fields such as drug discovery, life sciences, food science, and agrochemicals and also in environmental studies. Particularly, in pharmaceutical industries, as well as other pharmaceutical areas such as toxicological investigations and drug quality control, the development of analytical methods for the enantioseparation is of great importance [8–11].

Separations of enantiomeric compounds have been achieved by different instrumental techniques such as high performance liquid chromatography (HPLC) [12–14], gas chromatography (GC) [15,16], supercritical and subcritical fluid chromatography (SFC and SubFC) [17,18], capillary electrophoresis (CE), and capillary electrochromatography (CEC) [19–21].

The use of cyclodextrins (CDs) as chiral selectors, either in native form or as derivatives, is the most frequently approach applied in the enantiomeric separations due to the fact that they have high chemical stability and do not absorb UV–vis radiation [22–25].

The luminescent techniques have been the most frequently used methodologies for determining both therapeutic and abuse drugs probably due to its excellent selectivity and the low detection limits [26].

In process control or quality control of chiral drugs, a rapid method for their determination is required in order to enable

* Corresponding author at: Área de Química Analítica, Chacabuco y Pedernera, San Luis 5700, Argentina. Tel.: +54 266 4425 385.
E-mail address: lfernand@unsl.edu.ar (L.P. Fernández).

0039-9140/$ - see front matter © 2012 Elsevier B.V. All rights reserved.
http://dx.doi.org/10.1016/j.talanta.2012.11.045

analysis of large number of samples. In this context, flow injection analysis (FIA) would be ideal for achieving these requirements, due to its speed and simplicity. Therefore, a large number of FIA techniques combined with chemiluminescence, electrochemical, spectrophotometric and spectrofluorimetric detection methods have been reported [27,28].

Taking into account the need of simultaneously considering different aspects of the analysis, multifactor optimization was developed [29]. In order to carry out this type of study, experimental designs is a useful approach, specifically response surface analysis [30,31].

In this paper, we describe a flow injection-solid phase extraction (FI-SPE) with fluorescence detection for the enantioseparation of (±)-chlorpheniramine (CPA) using a microcolumn packed with a few milligrams of MWCNT. β-cyclodextrin was assayed as chiral selector in order to improve the ability of MWCNT on enantioseparation. The use of SDS as selective eluent was also evaluated. A multivariate study including a screening phase and a response surface method was used to optimize the overall method aiming to achieve adequate enantioresolution.

2. Experimental

2.1. Instrumental

All experiments were carried out on a Shimadzu RF-5301PC spectrofluorimeter (Shimadzu Corporation, Analytical Instrument Division, Kyoto Japan), equipped with a high-intensity Xenon discharge lamp. For the fluorescent measurements, 1-cm quartz cells were used in off-line assays and for flow measurements a LC flow-cell unit of 12 μL was used.

A model-5020 six-port two-way rotary valve from Rheodhyne (Rohnert Park, CA, USA) was used to set up the FIA manifold.

Two Minipuls 3 peristaltic pumps from Gilson (Villiers, France) with 1.3-mm ID Tygon pumping tubing to propel the reagents and samples (Middleton, WI, USA), were used.

A Model EA 940 Orion Expandable Ion Analyzer pH meter from Orion Research (Cambridge, MA, USA) with combined glass electrode was used.

2.2. Reagents

All the reagents were of analytical-reagent or spectroscopic grade. Chlorpheniramine maleate salts, and β-cyclodextrin were purchased from Sigma Chemical Co. (St. Louis, MO), sodium dodecylsulfate (SDS) was purchased from Tokyo Kasei Industries (Chuo-Ku, Tokyo, Japan). MWCNTs were purchased from Sigma Chemical Co. (St. Louis, MO). All other reagents and solvents were of analytical grade.

2.3. Solutions

(±)-Chlorpheniramine standard solution containing 10 mmol L^{-1} was prepared in water. This solution was stable for several weeks when was kept in dark at 5 °C. Standard working solutions of 1 mmol L^{-1} were prepared daily by stepwise dilutions with doubly distilled water.

The β-CD stock solution was prepared with double distilled water, to obtain a final concentration of 10 mmol L^{-1}. Solutions containing different β-CD:(±)-CPA ratios were obtained by suitably diluting with double distilled water.

A 0.02 mol L^{-1} SDS solution was prepared with an adequate weight of SDS and dissolving in double distilled water.

All solutions were degassed by ultrasound (Testlab, Argentina) before analysis.

2.4. MWCNTs activation

As it was demonstrated [32], effective oxidation of CNTs may be achieved when they are put in contact with HNO_3 2.0 mol L^{-1} overnight and raised with double distilled water to remove the excess of reactive, filtered throw filter paper (S&S blue band) and dried at ambient temperature. This procedure was followed in this work, and after the oxidation process they were stored into a desiccator until use.

2.5. Column preparation

A conical microcolumn was prepared by placing 10.0 mg of the nanomaterials based on previous results [28] into an empty 10-μL micropipette tip using the dry packing method described elsewhere [33]. To avoid filling losses when the sample solution passed through the conical microcolumn, a small amount of glass wool was placed at both ends. The final dimensions of the packed column were: 0.7 mm lower internal diameter and 1.2 mm upper internal diameter. The column was then connected to the peristaltic pump with Tygon tubing to form the flow injection system.

2.6. Experimental setup

A schematic diagram of the FI-SPE system is shown in Fig. 1. It includes two peristaltic pumps (**P**), a load/injection valve (**V**), a MWCNTs microcolumn (**mC**), and a flow cell (**D**) coupled to spectrofluorimetric detection. The overall procedure involves:

i) *Sample loading/background recording*: at the beginning, the mC was filled with the sample solution (line **S**) with valve **V** in load position (**a**). On the other hand, the mobile phase (HCl-SDS) flowed through the eluent (line **E**) to reach the detector and allowed baseline recording. This step took the time to

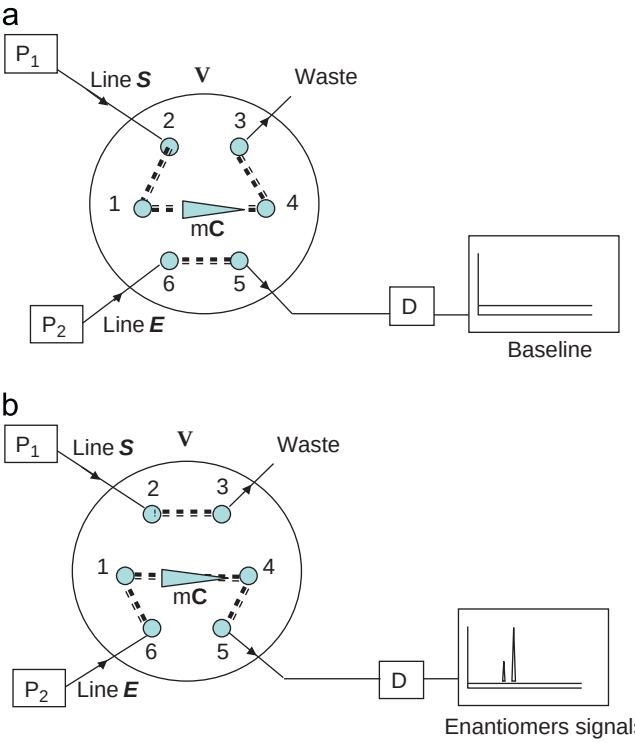

Fig. 1. Scheme of the FI-SPE manifold. **mC**, microcolumn; **P_1** and **P_2**, peristaltic pumps; **V**, load/injection valve (**a**, load position and **b**, injection position); **line *S***, sample line; **line *E***, eluent line and **D**, spectrofluorimeter.

load 1 mL of sample previously added with suitable amounts of β-CD, into the MWCNT mC.

ii) *Sample injection/data acquiring:* after the loading step, the valve **V** was switched to the injection position (**b**) allowing the mobile phase to pass through the mC and to elute the enantiomers.

iii) *Microcolumn washing/reconditioning step:* After data acquisition, the valve **V** remained in the injection position (**b**) for a duration of 1-min in order to condition the mC with the mobile phase. Afterwards, the valve is switched to position (**a**), and the sequence started again.

The experimental conditions were established and the separations were carried out operating in a time-course mode (transient signals; $\lambda_{exc}=240$ nm; $\lambda_{em}=370$ nm).

2.7. Software

Experimental design, data analysis and desirability function calculations were performed by using the software Stat-Ease Design-Expert trial Version 8.0.

2.8. Multivariate optimization

2.8.1. Screening phase: half-fraction factorial design (HFFD)

Experimental half-fraction factorial design is a factorial analysis involving ½ of the number of experiments of the full factorial design. This may be successfully applied with the aim to determine which variables mainly influence the enantioseparation. Moreover, a good experimental design provides a simple, efficient, and systematic approach to optimize designs for performance, quality and cost. Consequently, a HFFD was built for the evaluation of the main factors affecting the separation between (*R*)- and (*S*)-enantiomers, that may be quantified through the resolution *R*:

$$R=2(t_2-t_1)/(w_1+w_2) \quad (1)$$

where t_1 and t_2 are the elution times for each enantiomer, and w_1 and w_2 are the peak widths. When the resolution is higher than l.5, the two species are considered to be resolved at the baseline.

A two-level factorial design with $2^{(5-1)}=16$ experiments (Table 1) is described here for the variables: β–CD concentration, mmol L^{-1} (A); HCl concentration, mol L^{-1} (B); SDS concentration, mol L^{-1} (C); eluent flow-rate, rpm (D); and sample flow rate, rpm (E), while enantioresolution was the dependent variable. Maximum and minimum levels of the five variables were determined on the basis of preliminary studies. All experiments were performed in random order to minimize the effects of uncontrolled factors that may introduce bias on the measurements.

2.8.2. Optimization phase: central composite design (CCD)

Systematic optimization procedures are carried out by selecting an objective function, finding the most important factors and investigating the relationship between responses and factors by the so-called response surface methods (RSM). In the common way, a simple response is analyzed, and the model analysis indicates areas in the design region where the process is likely to give desirable results [29].

Once the conditions that ensure the enantioseparation were established, a spherical CCD was used here consisting of 30 experiments; i.e. combinations of 4 factorial points, 4 axial points, and 6 replicates of a central point. Experiments were combinations of the independent variables in the following ranges: β–CD concentration 1.0–3.0 mmol L^{-1}, HCl concentration 5.0×10^{-3}–1.0×10^{-2} mol L^{-1}; SDS concentration 4.0×10^{-4}–1.0×10^{-3} mol L^{-1} and eluent flow-rate 8–15 rpm (Table 2). The levels studied were selected considering the results of the HFFD. The enantioresolution (Eq. (1)) was thus fitted to a polynomial model and the maximum in the experimental domain was then obtained following the simplex optimization.

All experiments were performed in random order to minimize the effects of uncontrolled factors that may introduce bias in the measurements.

3. Results and discussion

3.1. Fluorimetric study of the analyte

The excitation and emission conditions for CPA were optimized in the common way, the wavelengths selected being 220 nm and 365 nm respectively. However, it was verified that

Table 1
Half design built for factor selection.

Experiment	*A*=[CD][a]	*B*=[HCl][b]	*C*=[SDS][c]	*D*=EFR[d]	*E*=SFR[d]	Enantioresolution[e]
1	3.0	0.01	50	15	15	0.83
2	0.5	0.001	10	5	15	0.39
3	0.5	0.01	10	5	5	2.34
4	3.0	0.001	50	5	15	1.34
5	0.5	0.01	50	15	5	1.00
6	3.0	0.001	10	15	15	1.12
7	3.0	0.01	10	5	15	2.00
8	0.5	0.001	50	5	5	0.32
9	0.5	0.001	10	15	5	0.58
10	3.0	0.01	10	15	5	1.43
11	3.0	0.01	50	5	5	1.28
12	0.5	0.01	50	5	15	1.14
13	0.5	0.01	10	15	15	0.62
14	3.0	0.001	10	5	5	1.28
15	0.5	0.001	50	15	15	4.47
16	3.0	0.001	50	15	5	1.43

[a] mmol L^{-1}.
[b] mol L^{-1}.
[c] mol L^{-1}.
[d] rpm.
[e] Eq. (1).

Table 2
Central composite design used for the optimization of enantioresolution.

Experiment	A=[CD][a]	B=[HCl][b]	C=[SDS][c]	D=EFR[d]	R
1	3	0.005	0.001	15	1.4
2	2	0.0075	0.0007	11.5	1.1
3	1	0.005	0.0004	8	1.7
4	2	0.0075	0.0001	11.5	0.9
5	3	0.01	0.001	8	0.9
6	2	0.0125	0.0007	11.5	1.0
7	1	0.005	0.0004	15	1.3
8	2	0.0075	0.0007	11.5	1.2
9	3	0.01	0.001	15	0.4
10	1	0.005	0.001	15	1.0
11	1	0.005	0.001	8	0.9
12	3	0.005	0.001	8	0.9
13	1	0.01	0.0004	15	1.6
14	2	0.0075	0.0007	11.5	1.2
15	2	0.0075	0.0013	11.5	1.4
16	2	0.0075	0.0007	11.5	1.2
17	3	0.01	0.0004	8	1.6
18	2	0.0075	0.0007	4.5	1.2
19	1	0.01	0.0004	8	2.1
20	1	0.01	0.001	8	1.0
21	4	0.0075	0.0007	11.5	0.8
22	2	0.0075	0.0007	11.5	1.2
23	1	0.01	0.001	15	1.6
24	2	0.0025	0.0007	11.5	0.8
25	3	0.005	0.0004	8	2.0
26	2	0.0075	0.0007	18.5	1.0
27	2	0.0075	0.0007	11.5	1.0
28	0	0.0075	0.0007	11.5	0.9
29	3	0.005	0.0004	15	1.2
30	3	0.01	0.0004	15	0.9

[a] mmol L^{-1}.
[b] mol L^{-1}.
[c] mol L^{-1}.
[d] rpm.

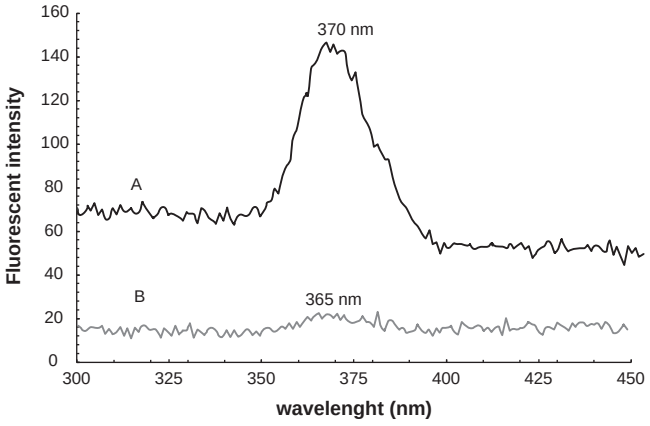

Fig. 2. Emission spectra for: **A**, 1.0 mmol L^{-1} (±)-chlorpheniramine–cyclodextrin complex (λ_{exc}=240 nm) and **B**, 1.0 mmol L^{-1} (±)-chlorpheniramine solution (λ_{exc}=220 nm).

CPA is weakly fluorescent under these conditions. Since CPA form an inclusion complex with β-CD [34], the spectroscopic conditions were re-optimized in presence of this reagent. The outcomes indicate that despite β-CD did not show fluorescence emission itself, the complex formation modifies the fluorescence behavior of both CPA enantiomers. As can be observed in Fig. 2, the emission spectra of CPA-β-CD complex (A) shows a little bathochromic shift to 370 nm (λ_{exc}=240 nm) accomplished by a notable enhancement of intensity fluorescence with respect to CPA (B).

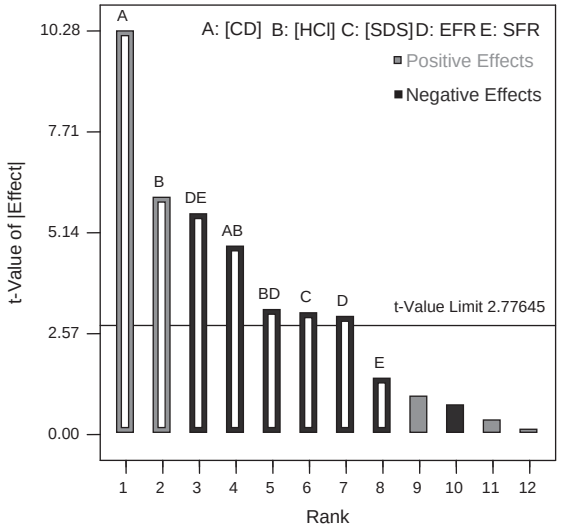

Fig. 3. Pareto chart for the studentized effects.

3.2. Half-fraction factorial design

The key factors selected during the optimization process were: β-CD concentration (factor A, [CD]); HCl concentration (factor B, [HCl]); SDS concentration (factor C, [SDS]); eluent (factor D, EFR) and sample (factor E, SFR) flow rates. These factors were evaluated at two levels each as discussed above (Table 1). The evaluation consisted in analyzing stock standard solutions in all cited conditions.

ANOVA tests (data shown as supplementary material) were applied to the experimental data in order to establish if the factors studied showed significant effects ($p<0.05$) on the analytical response R (calculated as discussed above). It could be laid out that the enantioresolution was negatively affected by EFR (p=0.040) and [SDS] (p=0.036), and positively affected by [HCl] (p=0.004) and [β-CD] (p=0.0005). As it was expected, the sample flow rate did not affect the resolution significantly (p=0.225) and because of that, it was fixed at 10 rpm (central value within the interval assayed). In order to get a deeper insight, a Pareto chart for the analyzed response was plotted, allowing reaching similar conclusions (Fig. 3). On the light of the experimental observations, it may be postulated that the enantioresolution may be a consequence of a synergism among the chiral edges of the nanomaterial, the β-CD and the mobile phase used for the elution.

3.3. Central composite design (CCD)

At this point it is evident that the HFFD enabled the discrimination amongst the most significant factors, though an accurate interpretation of those effects over the analytical response was not feasible. To this aim, a multilevel design was applied.

As it was discussed, RSMs allow defining empirically, once the conditions that ensure the enantioseparation were established, how responses behave at all values of the studied variables in the experimental domain [30]. In order to obtain the optimal conditions, a CCD was built, in which each design variable was assayed in the ranges mentioned in Section 2.8.2. The experimental matrix defined for the factors previously selected in the HFFD is shown in Table 2.

Polynomial models were used to fit the response for all the 30 experiments once outliers were removed by analyzing the externally studentized residuals (see Table 2) [30]. The model coefficients were calculated by backward multiple regression, and validated by the analysis of variance (ANOVA). In all cases,

irrelevant terms were eliminated (alpha > 0.1), although some of them were maintained to ensure hierarchy. The outcomes indicated that a reduced quadratic model represented better the behavior to enantioresolution with regard to the analyzed factors and in the levels studied. As can be observed, most model terms are significant ($p < 0.05$) and the lack of fit was not significant (Table 3).

The optimization procedure was thus carried out and the response surfaces were obtained. The CCD model yields a polynomial equation (showed as supplementary material) in which the model terms are preceded by the adjusted coefficients, including the intercept. One can conclude from the linear terms that, as in the HFD, the factors [CD] and [HCl] affect the enantioresolution positively whilst [SDS] showed negative influence.

Fig. 4 shows the enantioresolution as a function of the individual factors under study, while maintaining the others at their optimal values.

The experimental conditions corresponding to one maximum (enantioresolution = 2.13) are: [β-CD] = 1.0 mmol L^{-1}, [HCl] = 1.00×10^{-2} mol L^{-1}, [SDS] = 4.00×10^{-4} mol L^{-1} and EFR = 8.00 rpm.

These conditions were determined through a simplex optimization using the design points as starting conditions. Ten solutions were suggested, predicting values between 1.76 and 2.12 for enantioresolution. The suggested values during the optimization procedure were experimentally corroborated, and the corresponding FIAgram is shown in Fig. 5.

Table 3
ANOVA table for the reduced quadratic model fitted for enantioresolution.

Model term	Sum of squares	Degrees of freedom	Mean square	*F*-value	*p*-value Prob > *F*
[CD]	0.0191	1	0.0191	3.61926126	0.0795
[HCl]	0.091	1	0.0901	17.0725182	0.0012
[SDS]	0.7155	1	0.7155	135.626421	< 0.0001
EFR	0.0216	1	0.0216	4.09139141	0.0642
[CD]:[HCl]	0.3629	1	0.3629	68.7917623	< 0.0001
[CD]:[SDS]	0.1305	1	0.1305	24.7409639	0.0003
[CD]:EFR	0.0431	1	0.0431	8.17480404	0.0134
[HCl]:[SDS]	0.0456	1	0.0456	8.64348933	0.0115
[SDS]:EFR	0.9491	1	0.9491	179.9025	< 0.0001
$[CD]^2$	0.1140	1	0.1140	21.6051921	0.0005
$[HCl]^2$	0.0771	1	0.0771	14.6153217	0.0021
$[SDS]^2$	0.5450	1	0.5450	103.300597	< 0.0001
Residual	0.0685	13	0.0053		
Lack of Fit	0.0296	8	0.0037	0.47496687	0.8332

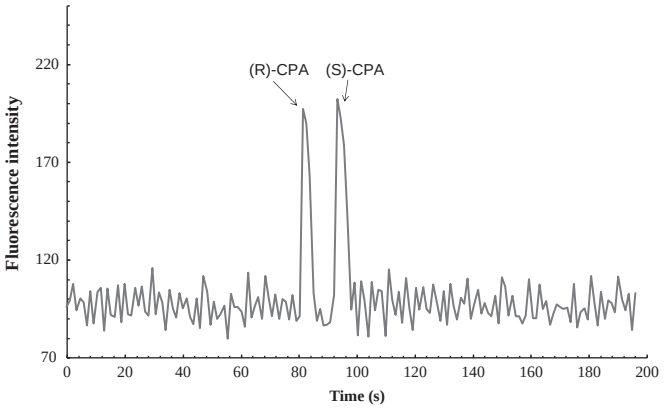

Fig. 5. Transient signal (FIAgram) obtained under optimized conditions corresponding to a baseline enantioresolution.

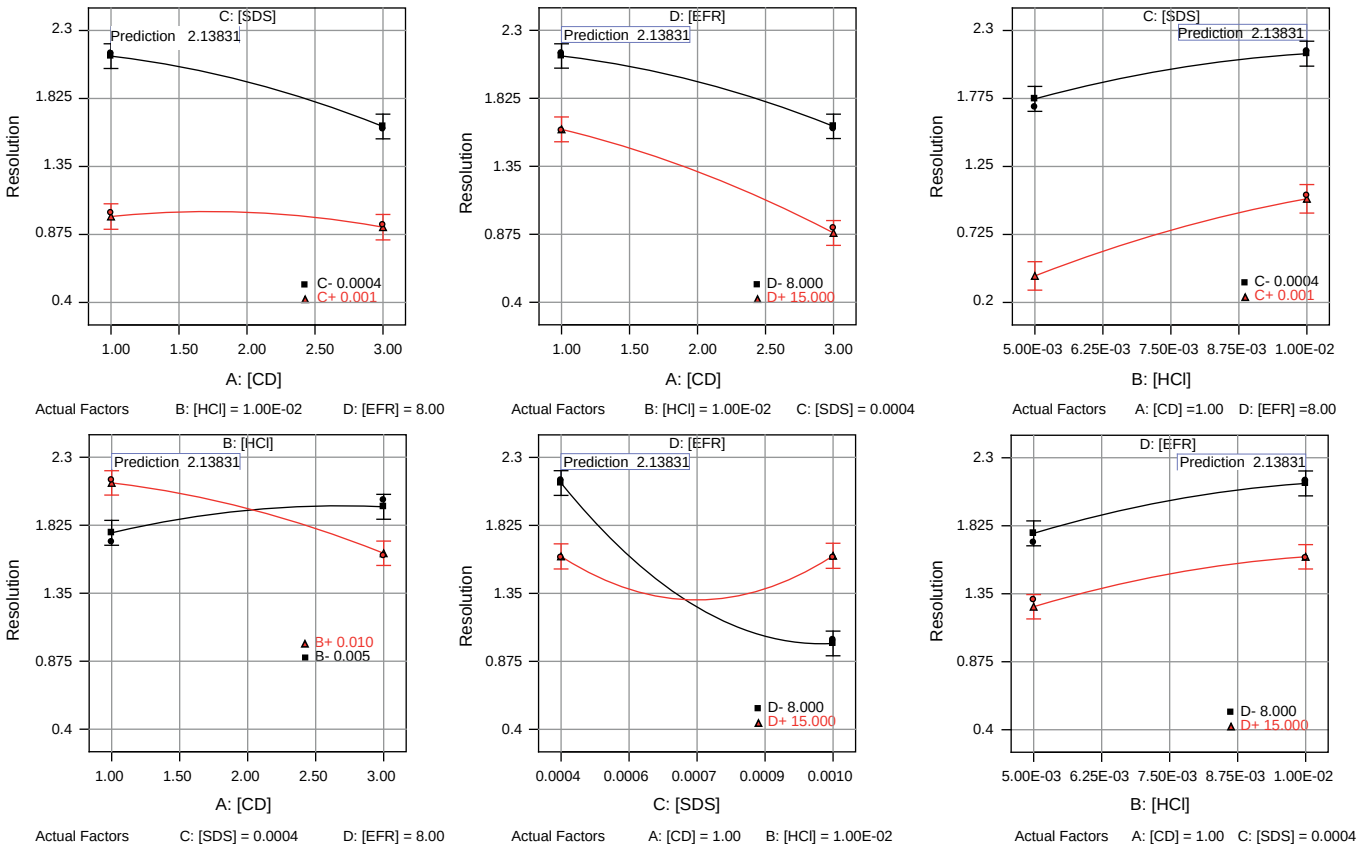

Fig. 4. 2-D plots of the enantioresolution as a function of two individual factors.

3.4. Method performance

An adequate enantioresolution (2.08) with satisfactory responses for both (*R*)-CPA (peak area=285) and (*S*)-CPA (peak area=380) was successfully achieved applying the proposed FI-SPE .

Once baseline resolution was achieved, the elution order (peak identity) was carried out through the analysis of (±)-CPA solution spiked with the pure enantiomers.

The intra-assay precision (repeatability) was determined by analysis of six replicate solutions under the same conditions, by the same analyst, and on the same day. The percent relative standard deviation (RSD%) value obtained while computing the enantioresolution calculated as indicated in Eq. (1) was 4.09%.

4. Conclusions

In this work, a SPE strategy that joins the chiral properties of MWCNTs and CD was designed to achieve resolution of chiral drugs. The overall methodology involved a FI separation process coupled to spectrofluorimetric detection. (±)-CPA was used as model drug and experimental variables that influence on resolution were optimized by the application of a multivariate design approach. This chemometric strategy represents a useful tool for the development of analytical methodologies in which many experimental parameters may be simultaneously optimized. Additionally, the implementation of straightforward enantioselective methodologies constitutes a valuable contribution to the field of the separation sciences.

Acknowledgments

This work was supported by Consejo Nacional de Investigaciones Científicas y Técnicas (CONICET); Agencia Nacional de Promoción Científica y Tecnológica (FONCYT, PICT-BID) and Universidad Nacional de San Luis (Argentina).

Appendix A. Supporting information

Supplementary data associated with this article can be found in the online version at http://dx.doi.org/10.1016/j.talanta.2012.11.045.

References

[1] Z. Liu, X. Sun, N. Nakayama-Ratchford, H. Dai, ACS Nano 1 (2007) 50–56.
[2] G.P. Rao, C. Lu, F. Su, Sep. Purif. Technol. 58 (2007) 224–231.
[3] K. Malek, R.A. van Santen, J. Membr. Sci. 311 (2008) 192–199.
[4] A.V. Herrera-Herrera, M.Á. González-Curbelo, J. Hernández-Borges, M.Á. Rodríguez-Delgado, Anal. Chim. Acta 734 (2012) 1–30.
[5] C. Chang, X. Wang, Y. Bai, H. Liu, Trends Anal. Chem. 39 (2012) 195–206.
[6] G. Gübitz, M.G. Schmid, J. Chromatogr. A 1204 (2008) 140–156.
[7] L. Zhao, P. Ai, A-H . Duan, L-M . Yuan, Anal. Bioanal. Chem. 399 (2011) 143–147.
[8] G. Alves, I. Figueiredo, M. Castel-Branco, A. Loureiro, A. Falcão, M. Caramona, Anal. Chim. Acta 596 (2007) 132–140.
[9] M.A. Tonon, P.S. Bonato, Electrophoresis 33 (2012) 1606–1612.
[10] H. John, F. Eyer, T. Zilker, H. Thiermann, Anal. Chim. Acta 680 (2010) 32–40.
[11] F.J. Malagueño de Santana, P.S. Bonato, Anal. Chim. Acta 606 (2008) 80–91.
[12] H. Ates, D. Mangelings, Y. Vander Heyden, J. Pharm. Biomed. Anal. 48 (2008) 288–294.
[13] S.K Thamarai Chelvi, E.L Yong, Yinhan Gong, J. Chromatogr. A 1203 (2008) 54–58.
[14] Y. Vander Heyden, D. Mangelings, N. Matthijs, C. Perrin, in: S. Ahuja, M.W. Dong (Eds.), Chiral Separations in Handbook of Pharmaceutical Analysis by HPLC, Elsevier, Amsterdam, 2005, pp. 447–498.
[15] V. Schurig, J. Chromatogr. A 906 (2001) 275–299.
[16] G.S. Ding, A.N Tang, J. Chromatogr. A 1208 (2008) 232–238.
[17] G. Terfloth, J. Chromatogr. A 906 (2001) 301–307.
[18] N. Byrne, E. Hayes-Larson, W. Liao, C.M. Kraml, J. Chromatogr. B 875 (2008) 237–242.
[19] A. Fayed, S. Weshahy, M. Shehata, N. Hassan, J. Pauwels, J. Hoogmartens, A. Van Schepdael, J. Pharm. Biomed. Anal. 49 (2009) 193–200.
[20] S. Fanali, G. D'Orazio, K. Lomsadze, B. Chankvetadze, J. Chromatogr. B 875 (2008) 296–303.
[21] D. Mangelings, C. Perrin, D.L. Massart, M. Maftouh, S. Eeltink, W. Kok, W.P.J. Schoenmakers, Y. Vander Heyden, Anal. Chim. Acta 509 (2004) 11–19.
[22] W. Lian, J. Huang, J. Yu, X. Zhang, Q. Lin, X. He, X. Xing, S. Liu, Food Control 26 (2012) 620–627.
[23] K. Nemeth, E. Varga, R. Ivanyi, J. Szeman, J. Visy, L. Jicsinszky, L. Szente, E. Forro, F. Fulop, A. Peter, M. Simonyi, J. Pharm. Biomed. Anal. 53 (2010) 382–388.
[24] H. Yang, Y. Zhu, D. Chen, C. Li, S. Chen, Z. Ge, Biosens. Bioelectron. 26 (2010) 295–298.
[25] E. Khaled, M.S Kamel, H.N.A. Hassan, A.A. Haroun, A.M. Youssef, H.Y. Aboul-Enein, Talanta 97 (2012) 96–102.
[26] T. Maki, N. Soh, K. Nakano, T. Imato, Talanta 85 (2011) 1730–1733.
[27] P. Fanjul-Bolado, P.J. Lamas-Ardisana, D. Hernández-Santos, A. Costa-García, Anal. Chim. Acta 638 (2009) 133–138.
[28] R.A. Silva, M.C. Talío, M.O. Luconi, L.P. Fernández, J. Pharm. Biomed. Anal. 70 (2012) 631–635.
[29] D.L. Massart, B.G.M. Vandeginste, S.N. Deming, Y. Michotte, L. Kaufman, Chemometrics: A textbook, Elsevier Amsterdam, 1988.
[30] L. Vera-Candioti, A.C. Olivieri, H.C. Goicoechea, Anal. Chim. Acta 595 (2007) 310–318.
[31] R.H. Myers, D. Montgomery, Response Surface Methodology, JohnWiley & Sons Inc., New York, 1995.
[32] J.W. Shim, S.J. Park, S.K. Ryu, Carbon N Y 39 (2001) 1635–1642.
[33] R.A. Gil, S.N. Goyanes, G. Polla, P. Smichowski, R.A. Olsina, L.D. Martinez, J. Anal. At. Spectrom. 22 (2007) 1290–1295.
[34] V.A. Bustos, G. Acosta, M.R. Gomez, V.D. Pereyra, Physica A 391 (2012) 4389–4396.